A COUPLED PRESSURE BASED SOLUTION ALGORITHM BASED ON THE VOLUME-OF-FLUID APPROACH FOR TWO OR MORE IMMISCIBLE FLUIDS

Kathrin Kissling[*]**, Julia Springer**[**]**, Hrvoje Jasak**[***]**, Steffen Schütz**[*]**, Karsten Urban**[**]**, Manfred Piesche**[*]

[*]Institute of Mechanical Process Engineering, University of Stuttgart, Germany
e-mail: kissling@imvt.uni-stuttgart.de
[**]Institute of Numerical Mathematics, University of Ulm, Germany
e-mail: julia.springer@uni-ulm.de
[***]Wikki Ltd., London, United Kingdom
e-mail: h.jasak@wikki.co.uk

Key words: Multiphase flow, Volume-of-Fluid, coupled solution approach

Abstract. *The purpose of this study is to describe a coupled pressure based solution algorithm to model interface capturing problems for multiphase flows where neither of the phases can be regarded as dominant. As to a segregated approach using an iterative solution scheme consisting of successive solutions of the transport equation for each phase, the phase for which the equation is solved first dominates the phases for which the transport equations are solved later. This is the result of the requirement of a bounded solution for the phase fraction variables. A cell which is already completely filled with one phase cannot contain any more fluid of any other phase. In the present study, a coupled solution approach of the equations to describe the transport of the phases and the pressure equation is presented. This coupled approach avoids the predescribed numerically induced predominance of a single phase which may occur if a common segregated algorithm is used.*

The system is described by the continuity equation, the equations to model the transport of the volume fractions α_i and the volumetrically averaged momentum equation. By analogy with the derivation of the pressure equation in PISO or SIMPLE, the discretised momentum balance is inserted in the equations to describe the transport of the N phases. While the volume fractions of $(N-1)$ phases are gained by solving the transport equations, the volume fraction of the N-th phase is calculated by applying the closure equation.

In contrast to segregated approaches, the equations for pressure and volume fractions are now solved simultaneously in one single step. Therefore the state variables can implicitly depend on other state variables. To achieve a strong coupling between the volume fractions and the pressure, the pressure is treated implicitly in the equations for the volume fractions and the volume fractions are equally treated implicitly in the pressure equation. The coupled approach with the additional implicit dependencies leads to a matrix which is larger and has more non-zero entries than the matrices of a segregated approach. Therefore the effort to solve the equation system increases significantly. The system is solved applying the block matrix implementation by Jasak.[1]

1 INTRODUCTION

Interface capturing is an active area of research in computational fluid dynamics. The current study deals with the problem of describing a multiphase flow system with more than one phase, where neither of the phases can be regarded as dominant. As to a segregated approach using an iterative solution scheme consisting of successive solutions of the transport equation for each phase, the phase for which the equation is solved first is dominating the phase for which the transport equation is solved later. This is a result of the requirement to preserve the boundedness of the volume fraction values. If a cell is already completely filled with one fluid, it cannot receive any more fluid of any other phase. If the MULES (Multidimensional Universal Limiter with Explicit Solution) solver, implemented in OpenFOAM®, is enhanced to model a system with more than two immiscible fluids, its structure enforces the dominant behaviour of the first phase. This is due to the fact that MULES clips the fluxes transporting the second phase in dependency of the value in the considered cell to avoid an unbounded solution. The following approach tries to avoid this phenomenon by introducing a better coupling of the equations.

In the following section 2 the governing equations that are used in the new coupled approach will be presented. In section 3 the numerical solution for these equations and its implementation will be described. Finally section 4 contains the results of different test cases.

2 GOVERNING EQUATIONS

The governing equations for this multiphase flow problem are the equation of continuity, momentum and of the transport of the volume fraction distributions. In the current study the fluid is assumed to be incompressible and Newtonian. Hence, the continuity equation reads

$$\nabla \cdot \mathbf{U} = 0 \tag{1}$$

and the momentum equation reads

$$\frac{\partial \rho \mathbf{U}}{\partial t} + \nabla \cdot (\rho \mathbf{U} \mathbf{U}) = -\nabla p + \nabla \cdot \boldsymbol{\tau} + \rho \mathbf{f} + \sum_{i=1}^{N} \sum_{k=i+1}^{N} \mathbf{F}_{ik}. \tag{2}$$

Here $\boldsymbol{\tau}$ describes the viscous stress tensor and $\mathbf{F}_{ik} = \int_{S(t)} \sigma_k \kappa \, \delta (\mathbf{x} - \mathbf{x}') \, dS$ is the influence on the momentum due to the surface tension forces of the interface between the phases indexed by i and k respectively. The surface tension force is only present at points $\mathbf{x}'$ of the free surface. This is ensured by the Dirac-δ-distribution. The number of phases is described by N. Further, $\mathbf{f}$ describes an arbitrary mass-related force, here the gravitational force. Density ρ and viscosity μ are treated as volumetric mixture values obtained by

$$\rho = \sum_{i=1}^{N} (\alpha_i \rho_i) \tag{3}$$

and

$$\mu = \sum_{i=1}^{N} (\alpha_i \mu_i). \tag{4}$$

The transport equation for the ith volume fraction α_i reads

$$\frac{\partial \alpha_i}{\partial t} + \nabla \cdot (\alpha_i \mathbf{U}) = 0. \tag{5}$$

The volume fractions α_i are coupled by the normalization:

$$\sum_{i=1}^{N} \alpha_i = 1, \quad \alpha_i \in [0, 1]. \tag{6}$$

To model the influence of the surface tension, the Continuum-Surface-Force Model of Brackbill[2] is used. Brackbill interpreted the surface tension as a continuous, three-dimensional effect across an interface. This approach is applied here since in interface-capturing methods the interface is neither tracked explicitly nor shape or location are known. Therefore, an exact boundary condition cannot be applied to the interface. Hence, the influence of the surface tension formulated as volumetric force reads:

$$\mathbf{F}_{ik} = \sigma_{ik} \kappa_{ik} (\nabla \alpha)_{ik}, \tag{7}$$

where $(\nabla \alpha)_{ik}$ is calculated as

$$(\nabla \alpha)_{ik} = \alpha_k \nabla \alpha_i - \alpha_i \nabla \alpha_k. \tag{8}$$

The curvature is defined as

$$\kappa_{ik} = \nabla \cdot \left(\frac{(\nabla \alpha)_{ik}}{|(\nabla \alpha)_{ik}|} \right), \tag{9}$$

where the unit normal vector $\mathbf{n}$ yields

$$\kappa_{ik} = -\nabla \cdot \mathbf{n}. \tag{10}$$

As only Newtonian fluids are modelled, the viscous stress tensor is given by

$$\boldsymbol{\tau} = \mu \left(\nabla \mathbf{U} + \nabla \mathbf{U}^T \right). \tag{11}$$

The divergence of the viscous stress tensor $\nabla \cdot \boldsymbol{\tau}$ can be reformulated as

$$\nabla \cdot \boldsymbol{\tau} = \nabla \cdot (\mu \nabla \mathbf{U}) + (\nabla \mathbf{U} \cdot \nabla \mu). \tag{12}$$

Moreover, the pressure p can be substituted by

$$p = p^* + \rho \mathbf{f} \cdot \mathbf{x}, \tag{13}$$

where $\rho \mathbf{f} \cdot \mathbf{x}$ represents the hydrostatic pressure. This leads to the equation

$$\frac{\partial \rho \mathbf{U}}{\partial t} + \nabla \cdot (\rho \mathbf{U} \mathbf{U}) = -\nabla p^* + \nabla \cdot (\mu \nabla \mathbf{U}) + (\nabla \mathbf{U} \cdot \nabla \mu) - \mathbf{f} \cdot \mathbf{x} \nabla \rho + \sum_{i=1}^{N} \sum_{k=i+1}^{N} \sigma_{ik} \kappa_{ik} (\nabla \alpha)_{ik}. \tag{14}$$

3 NUMERICAL SOLUTION

The following procedure is due to Weller[3,4] . It is reviewed here, since it is the basis of the derivation of our coupled solution method. The momentum equation is discretised not taking into account all terms that are proportional to $(\nabla \alpha)_{ik}$ or ∇p. The resulting system of linear algebraic equations is denoted by

$$\boldsymbol{\mathcal{A}} := \left\{ \left[\frac{\partial \rho\left[\mathbf{U}\right]}{\partial t} \right] + \left[\nabla \cdot \left(\rho_f \phi\left[\mathbf{U}\right]_f \right) \right] = \left[\nabla \cdot \left(\mu_f \nabla\left[\mathbf{U}\right] \right) \right] + \left(\nabla \mathbf{U}\right) \cdot \nabla \mu_f \right\}, \qquad (15)$$

where $[\cdot]$ stands for an implicit discretisation operator and the index f denotes values at the cell faces. Note that $\boldsymbol{\mathcal{A}}$ contains the full system of equations $\mathbf{AU} = \mathbf{b}$ including the matrix $\mathbf{A}$, the vector $\mathbf{U}$ of unknown velocities and the source vector $\mathbf{b}$.

This system of equations can further be reformulated with the use of some operators acting on $\boldsymbol{\mathcal{A}}$. The following operators are provided in the library lduMatrix within the OpenFOAM® distribution:

- the D-Operator defined as $\boldsymbol{\mathcal{A}}_D := \mathrm{diag}\left(\mathbf{A}\right)$,

- the N-Operator as $\boldsymbol{\mathcal{A}}_N := \mathbf{A} - \mathrm{diag}\left(\mathbf{A}\right)$,

- the S-Operator which is $\boldsymbol{\mathcal{A}}_S := \mathbf{b}$ and

- the H-Operator $\boldsymbol{\mathcal{A}}_H := \mathbf{b} - \boldsymbol{\mathcal{A}}_N \mathbf{U} = \boldsymbol{\mathcal{A}}_D \mathbf{U}$

With these operators at hand, the linear equation system $\boldsymbol{\mathcal{A}}$ can be written as

$$\left(\boldsymbol{\mathcal{A}}_D + \boldsymbol{\mathcal{A}}_N\right) \mathbf{U} = \boldsymbol{\mathcal{A}}_S. \qquad (16)$$

for the solution vector $\mathbf{U}$.[4] This leads to the semi-discretised form of the momentum equation

$$\boldsymbol{\mathcal{A}}_D \mathbf{U} = \boldsymbol{\mathcal{A}}_H - \nabla p^* - \mathbf{f} \cdot \mathbf{x} \nabla \rho + \sum_{i=1}^{N} \sum_{k=i+1}^{N} \sigma_{ik} \kappa_{ik} \left(\nabla \alpha\right)_{ik}. \qquad (17)$$

A rearrangement yields

$$\mathbf{U} = \frac{\boldsymbol{\mathcal{A}}_H}{\boldsymbol{\mathcal{A}}_D} - \frac{\nabla p^*}{\boldsymbol{\mathcal{A}}_D} - \frac{\mathbf{f} \cdot \mathbf{x} \nabla \rho}{\boldsymbol{\mathcal{A}}_D} + \frac{\sum_{i=1}^{N} \sum_{k=i+1}^{N} \sigma_{ik} \kappa_{ik} \left(\nabla \alpha\right)_{ik}}{\boldsymbol{\mathcal{A}}_D}. \qquad (18)$$

Since velocity and pressure are normally solved in a segregated approach, an iterative scheme is used which starts with the flux predictor ϕ^* which is later corrected in order to obtain the flux ϕ after having solved the pressure equation. By interpolating the momentum equation with central differences the flux predictor and corrector can be obtained by

$$\phi = \phi^* - \left(\frac{1}{\boldsymbol{\mathcal{A}}_D}\right) |\mathbf{S}| \, \nabla_f^{\perp} p^*. \qquad (19)$$

Here, the operator $\nabla_f^\perp$ denotes the gradient normal to the cell faces and $|\mathbf{S}|$ is the magnitude of the area vector of the regarded cell face. In this equation, the first term on the right-hand side ϕ^* can be formulated as

$$\phi^* = \left(\frac{\boldsymbol{\mathcal{A}}_H}{\boldsymbol{\mathcal{A}}_D}\right)_f \cdot \mathbf{S} - \left(\frac{1}{\boldsymbol{\mathcal{A}}_D}\right)_f (\mathbf{f} \cdot \mathbf{x})_f \, |\mathbf{S}| \, \nabla_f^\perp \rho + \sum_{i=1}^N \sum_{k=i+1}^N \left(\left(\frac{1}{\boldsymbol{\mathcal{A}}_D}\right)_f (\sigma_{ik}\kappa_{ik})_f \, |\mathbf{S}| \, \left(\nabla_f^\perp \alpha\right)_{ik}\right). \tag{20}$$

The second term on the right-hand side of (19) is the flux corrector. The continuity equation is formulated at the cell faces and the flux is substituted into it. This yields

$$\nabla \cdot \phi = 0. \tag{21}$$

Inserting (19) into (21) and rearranging leads to the pressure equation:

$$\left[\nabla \cdot \left(\left(\frac{1}{\boldsymbol{\mathcal{A}}_D}\right)_f \nabla [p^*]\right)\right] = \nabla \cdot \phi^*. \tag{22}$$

The equation describing the transport of the volume fraction is taken and reformulated according to Weller,[3] resulting in conservative forms of all terms. Note that, since $\alpha_i \in [0, 1]$, $1 \leq i \leq N$, the terms are bounded from below and above. For a two-phase system, this equation reads:

$$\frac{\partial \alpha_1}{\partial t} + \nabla \cdot (\mathbf{U}\alpha_1) + \nabla \cdot (\mathbf{U}_r \alpha_1 \alpha_2) = 0, \tag{23}$$

where $\mathbf{U}_r$ describes the relative velocity at the free surface. It can be modelled as

$$\mathbf{U}_r = \min\left(c_\alpha \, |\mathbf{U}|, \max\left(|\mathbf{U}|\right)\right) \cdot \mathbf{n}, \tag{24}$$

where c_α is the compression coefficient for the interface. (See Weller[3] for details.) After discretisation it reads:

$$\left[\frac{\partial [\alpha_1]}{\partial t}\right] + \left[\nabla \cdot (\mathbf{U}\alpha_1)\right] + \left[\nabla \cdot (\mathbf{U}_r \alpha_1 \alpha_2)\right] = 0 \tag{25}$$

For multiphase-systems the same reformulation leads to

$$\frac{\partial \alpha_i}{\partial t} + \nabla \cdot (\mathbf{U}\alpha_i) + \nabla \cdot \left(\alpha_i \sum_{k=1, k\neq i}^N \alpha_k \mathbf{U}_{r,ik}\right) = 0, \tag{26}$$

where $\mathbf{U}_{r,ik}$ is the relative velocity between the phases i and k. The next step is to restrict (26) to the cell faces. Hence an equation for the volumetric flux on the cell faces is obtained. The equation is discretised yielding

$$\left[\frac{\partial [\alpha_i]}{\partial t}\right] + \left[\nabla \cdot \left(\phi [\alpha_i]_f\right)\right] + \left[\nabla \cdot \left([\alpha_i]_f \sum_{k=1, k\neq i}^N \alpha_{k,f} \phi_{r,ik}\right)\right] = 0. \tag{27}$$

Since the volumetric mixture flux ϕ satisfies the continuity of the mixture velocity $\mathbf{U}$, the second term is bounded in $[0, 1]$. Problems for the boundedness of the variables arise from the

third term. The bounding of α_i is achieved by using the relative face flux $\phi_{r,ik}$ to interpolate α_i to the face while $-\phi_{r,ik}$ is used to interpolate α_k to the face. Using First Order Upwind as a convection scheme, the solution is bounded, but might have a serious diffusivity while the usage of higher order convection schemes might reduce the numerical diffusion but impact the boundedness of the solution.[5] Moreover, the third term is nonlinear in α. The flux ϕ is defined as

$$\phi = \mathbf{S} \cdot \mathbf{U}_f, \tag{28}$$

but here a different approach is taken. Instead (19) and (20) of the pressure-velocity coupling are substituted into (27). In this way the flux predictor and the flux corrector are both taken into account. Furthermore, the value of the flux ϕ and the fulfilment of continuity are no longer dependent on the choice of the interpolation scheme.

$$
\begin{aligned}
\left[\frac{\partial [\alpha_i]}{\partial t} \right] &+ \left[\nabla \cdot \left(\left(\left(\frac{\mathcal{A}_H}{\mathcal{A}_D} \right)_f \cdot \mathbf{S} + \sum_{i=1}^{N} \sum_{k=i+1}^{N} \left(\left(\frac{1}{\mathcal{A}_D} \right)_f (\sigma_{ik}\kappa_{ik})_f |\mathbf{S}| \left(\nabla_f^{\perp} \alpha \right)_{ik} \right) \right. \right. \\
&\left. \left. - \left(\frac{1}{\mathcal{A}_D} \right)_f (\mathbf{f} \cdot \mathbf{x})_f |\mathbf{S}| \nabla_f^{\perp} \rho \right) [\alpha_i]_f \right) \right] \\
&- \left[\nabla \cdot \left(\left(\frac{1}{\mathcal{A}_D} \right)_f \nabla [p^*] \alpha_{i,f} \right) \right] + \left[\nabla \cdot \left([\alpha_i]_f \sum_{k=1,k\neq i}^{N} \alpha_{k,f} \phi_{r,ik} \right) \right] = 0.
\end{aligned}
\tag{29}
$$

In this equation, however, new terms appear that are nonlinear. In order to linearize those terms only one variable can be chosen to be treated implicitly while the other variables need to be treated explicitly. The first nonlinear term of the equation is

$$
\nabla \cdot \left(\left(\sum_{i=1}^{N} \sum_{k=i+1}^{N} \left(\left(\frac{1}{\mathcal{A}_D} \right)_f (\sigma_{ik}\kappa_{ik})_f |\mathbf{S}| \left(\nabla_f^{\perp} \alpha \right)_{ik} \right) \right) [\alpha_i]_f \right). \tag{30}
$$

In this term α_i is chosen to be treated implicitly, while all the other variables that appear in $\nabla_f^{\perp} \alpha$ are treated explicitly. The term

$$
\nabla \cdot \left(\left(\frac{1}{\mathcal{A}_D} \right)_f \nabla [p^*] \alpha_{i,f} \right) \tag{31}
$$

can be treated either explicitly in the pressure and implicitly in the volume fraction or vice versa. To achieve a better coupling between the equations the pressure is treated implicitly. In the last term

$$
\nabla \cdot \left([\alpha_i]_f \sum_{k=1,k\neq i}^{N} \alpha_{k,f} \phi_{r,ik} \right) \tag{32}
$$

it would be desirable to implicitly model α_k while keeping α_i explicit to strongly couple the volume fraction distributions. However, this is impossible since the diagonal dominance is seriously weakened, and convergence is no longer guaranteed. Therefore, the coupling between

the single phases is only achieved by the closure equation where all terms are treated implicitly. To achieve an additional coupling between the state variables, the flux predictor in the pressure equation is formulated in artificial dependency of the volume fractions:

$$\phi^* = \sum_{i=1}^{N} \alpha_i \phi^*. \tag{33}$$

The pressure equation for the coupled approach now yields:

$$\left[\nabla \cdot \left(\left(\frac{1}{\mathcal{A}_D} \right)_f \nabla \left[p^* \right] \right) \right] = \nabla \cdot \sum_{i=1}^{N} \left[\alpha_i \right] \phi^*. \tag{34}$$

The complete system reads:
1. Pressure equation:

$$\left[\nabla \cdot \left(\left(\frac{1}{\mathcal{A}_D} \right)_f \nabla \left[p^* \right] \right) \right] = \nabla \cdot \sum_{i=1}^{N} \left[\alpha_i \right] \phi^*. \tag{35}$$

2. Pressure based equation for the volume fractions:

$$
\left[\frac{\partial \left[\alpha_i \right]}{\partial t} \right] + \left[\nabla \cdot \left(\left(\left(\frac{\mathcal{A}_H}{\mathcal{A}_D} \right)_f \cdot \mathbf{S} + \sum_{i=1}^{N} \sum_{k=i+1}^{N} \left(\left(\frac{1}{\mathcal{A}_D} \right)_f (\sigma_{ik}\kappa_{ik})_f \left| \mathbf{S} \right| \left(\nabla_f^{\perp} \alpha \right)_{ik} \right) \right. \right.
$$
$$
\left. \left. - \left(\frac{1}{\mathcal{A}_D} \right)_f (\mathbf{f} \cdot \mathbf{x})_f \left| \mathbf{S} \right| \nabla_f^{\perp} \rho \right) \left[\alpha_i \right]_f \right) \right] \tag{36}
$$
$$
- \left[\nabla \cdot \left(\left(\frac{1}{\mathcal{A}_D} \right)_f \nabla \left[p^* \right] \alpha_{i,f} \right) \right] + \left[\nabla \cdot \left(\left[\alpha_i \right]_f \sum_{k=1, k \neq i}^{N} \alpha_{k,f} \phi_{r,ik} \right) \right] = 0.
$$

3. Closure equation:

$$\sum_{i=1}^{N} \left[\alpha_i \right] = 1. \tag{37}$$

3.1 THE BLOCK MATRIX STRUCTURE

In this section the implementation of the described system in OpenFOAM® with the use of the block matrix structure[1] is explained. Due to the previously mentioned discretisation we obtain equations for each cell which can be described in the following form

$$\mathbf{A}_i \mathbf{x}_i + \sum_{n} \mathbf{A}_n \mathbf{x}_n = \mathbf{b}_i, \tag{38}$$

where $\mathbf{x}_i$ are variable values in the considered cell and $\mathbf{x}_n$ are the variable values of the neighbour cells. Correspondingly, $\mathbf{A}_i$ describes the influence of the considered cell and therefore the diagonal elements while $\mathbf{A}_n$ describes the offdiagonals which couple the single cells with each neighbour. Finally, $\mathbf{b}_i$ is the explicit source term for the considered cell. In contrast to

a segregated approach, the equations for pressure and for the volume fractions are all solved simultaneously and can implicitly depend on other state variables. Therefore, the equations for pressure and the volume fractions in every cell form a system of equations in which $\mathbf{x}_i$ is not only a scalar variable value but a vector of length $(N+1)$ for the pressure value and the values of the volume fractions in the regarded cell. The values for the neighbour cells in $\mathbf{x}_n$ have the same structure. In the same way $\mathbf{A}_i$ and $\mathbf{A}_n$ are not only scalar coefficient values, but $(N+1) \times (N+1)$-matrices where all implicit dependencies of the equations are stored. Depending on the discretisation schemes the single terms are now distributed into the diagonals and the off-diagonals of the tensor $\mathbf{A}$. All the coefficients of the pressure equation are located in the first row and the coefficients for $(N-1)$ phase equations in the following rows. The last equation is the closure equation. Due to the coupled approach and the additional implicit dependencies the resulting matrix is larger and has more non-zero entries. Therefore, the effort to solve the equation system increases significantly. The block matrix structure in the implementation[1] stores the entries in three arrays, the diagonal, the lower triangle and the upper triangle. This is represented in Figure 1.
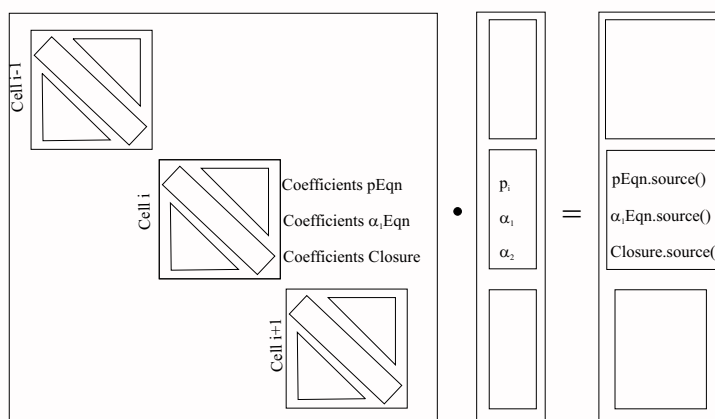

Figure 1: Representation of the block matrix structure

3.2 THE ALGORITHM

Now the full algorithm can be described in detail. The basic format resembles the SIMPLE (Semi-Implicit Method for Pressure-Linked Equations) algorithm[6] with the difference that the solution is obtained by simultaneously solving for pressure and volume fractions, as mentioned before. After the time loop has been started, the material properties in the mixture approach need to be updated to the actual distribution of the volumetric phase fractions, as described in (3) and (4). Next, the modified transient SIMPLE loop is started. The governing equations are established at this point, but not solved. In this way, the coefficients which are now fed into the block matrix structure are obtained. Using a GMRES (Generalized Minimal Residual) solver, the system is solved. The fluxes are corrected and the pressure is explicitly relaxed. The interfaces are corrected before the velocity is updated. Depending on the number of correctors for the SIMPLE loop, this procedure is repeated. The algorithm is visualised in Figure 2.
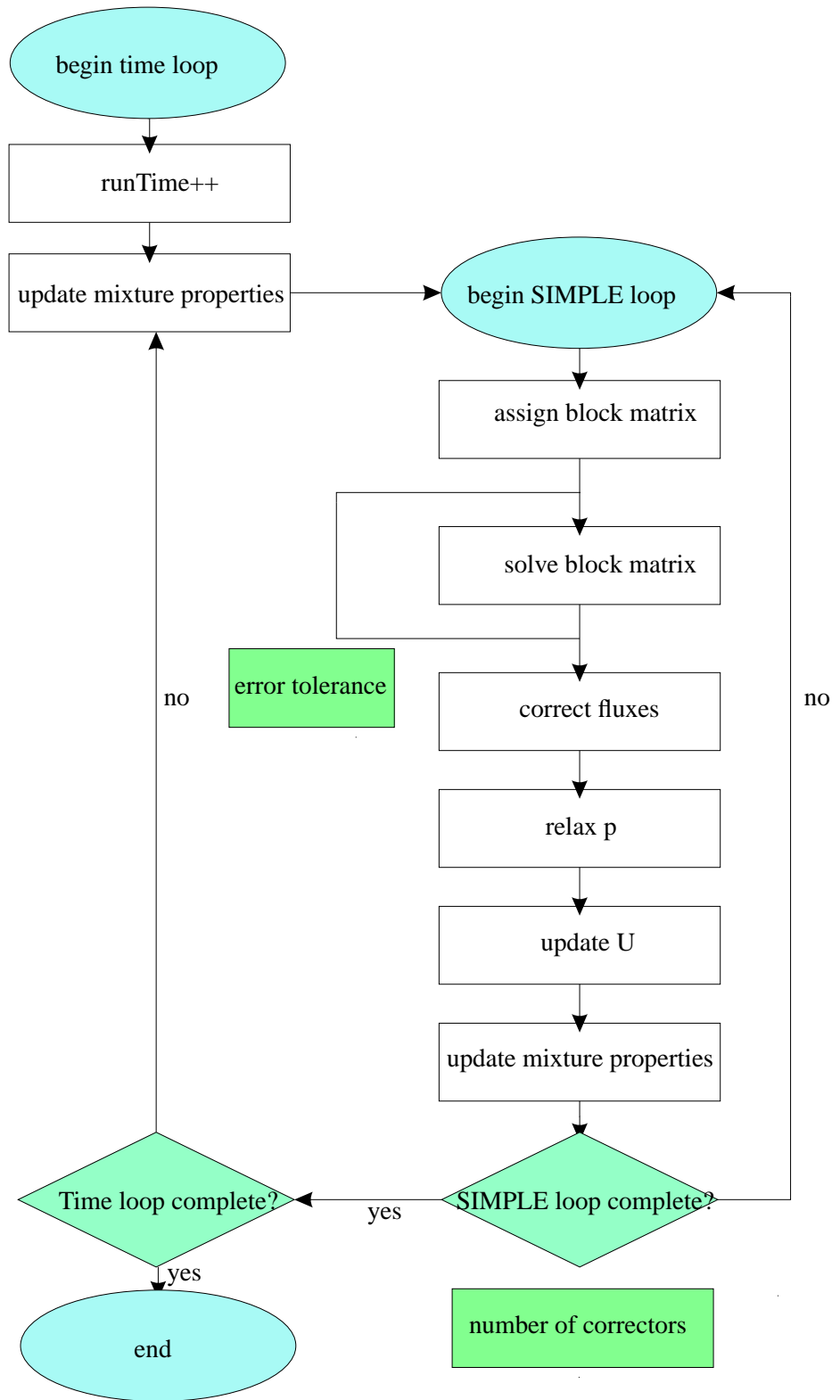
Figure 2: Solution algorithm

4 TEST CASES

The presented algorithm is validated regarding different test cases taken from literature. The first testcase describes the collapse of a liquid column.[7,8] A second test case covers sloshing of a liquid wave in a tank.[8,9] The last test case is presented to show the applicability of the concept to test cases with more than two phases as well as three dimensions. The case is similar to the first test case but with two collapsing liquid columns.

4.1 Collapse of a liquid column

A classical validation test case of the mathematical modelling of free surface flow is the collaps of a liquid column.[7,8] Unfortunately measurements of the exact interface conture are not available. However, Koshizuka[7] evaluated the speed of the wave and the reduction of the column height from photographs. The experiments were carried out in a glass tank with a base length of 0.584 m, while the water column has a base length of 0.146 m and a height of 0.292 m. Due to the gravitational acceleration, the water column collapses to seek the lowest level of potential energy. The dimensions are relatively large. Hence surface tension effects can be neglected. At first the flow is dominated by inertia forces. The viscous forces gain importance, when the flow is settling at the bottom of the tank. The glass walls have been modelled with no-slip boundary conditions. The numerical results for the velocity field and the position of the fluid at six different times are shown in Figure 3. Figures 4 and 5 show the numerical results compared to experimental results by Koshizuka.[7] The numerical results obtained with the coupled appoach are in excellent agreement with the experimental data. Therefore the coupled solution approach for pressure and volume fraction equations can be regarded as justified.

4.2 Sloshing of a liquid wave in a tank

The sloshing of a liquid wave in a tank is used as a test case since an analytical solution for the period of the sloshing wave exists. This case was first mathematically investigated by Tadjbakhsh and Keller[10] and applied as a test case for numerical simulations by Raad[9] and Ubbink.[8] The wave in the test case shows a low amplitude and the dominant acceleration force is the gravitational force. The test case enables the validation with respect to the numerical dissipation introduced by the discretisation and the ability of the method to conserve the energy of the system, especially during transfer of potential energy into kinetic energy and vice versa. The simulation setup consists of a tank with a base length of 100 mm and a height of 130 mm. The domain is uniformly discretised with 40 cells in the horizontal direction and 104 cells in the vertical direction resulting in $\delta_x = 0.625$ mm and $\delta_y = 1.25$ mm. The walls on the left, the right and the bottom sides of the domain are treated as slip boundaries whereas at the top an atmosphere boundary is specified. The fluid has an average depth of 50 mm. Its surface is initially defined by one half of a cosine wave with an amplitude of 5 mm. The densities of the fluids water and air are defined as $\rho_w = 1000 \text{kg/m}^3$ and $\rho_a = 1 \text{kg/m}^3$ respectively, while the viscosities are taken as zero. Due to the gravitational field, the fluid begins to slosh. The gravitational acceleration is set to 9.8 m/s^2. The first mode of the sloshing has the theoretical period of[9]

$$P = 2\pi \left[gk\tanh\left(kh\right) \right]^{-1/2} = 0.3739 \text{s} \tag{39}$$

t = 0.0 s

t = 0.2 s

t = 0.4 s

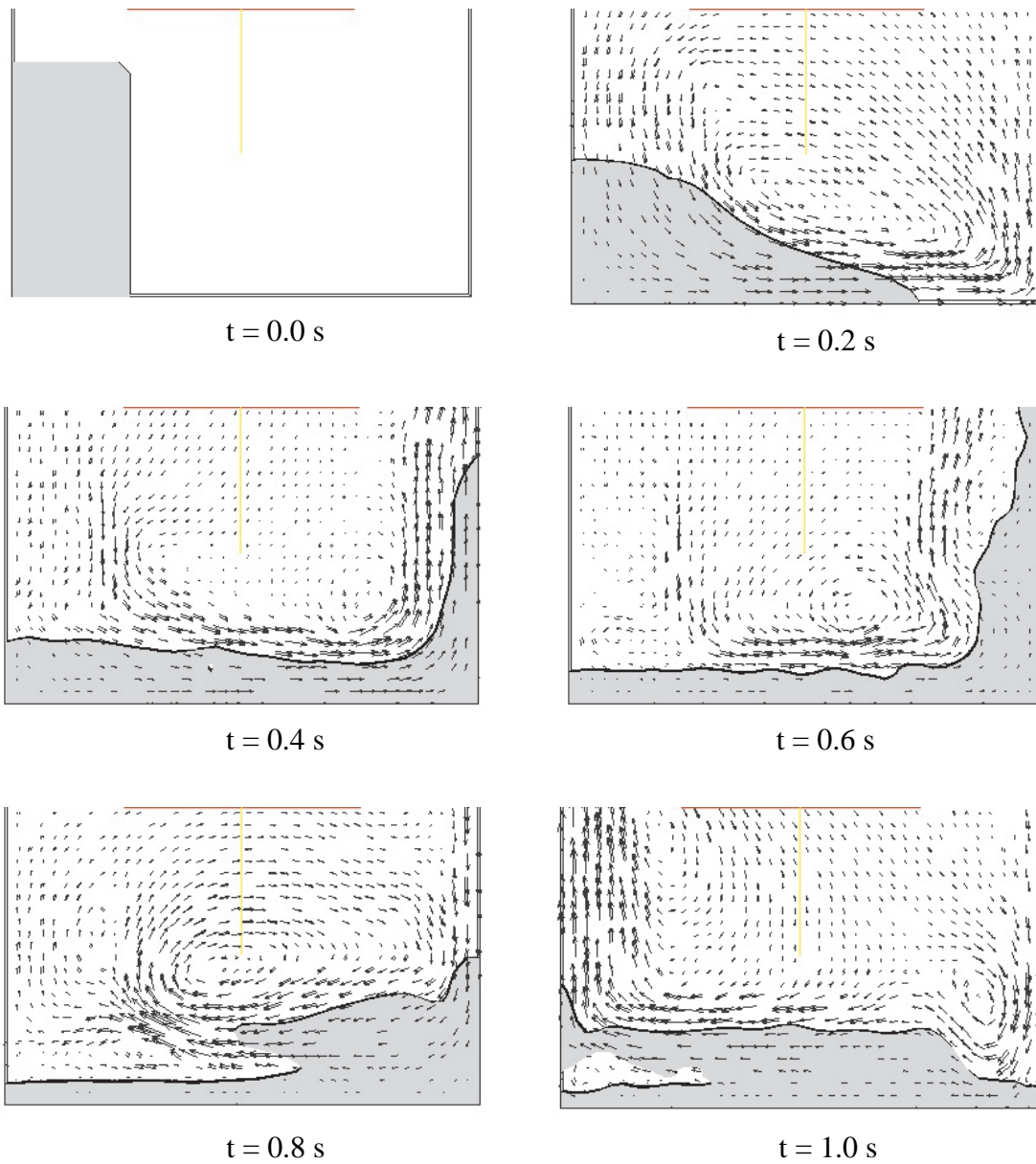t = 0.6 s

t = 0.8 s

t = 1.0 s

Figure 3: Numerical results of the collapsing water column
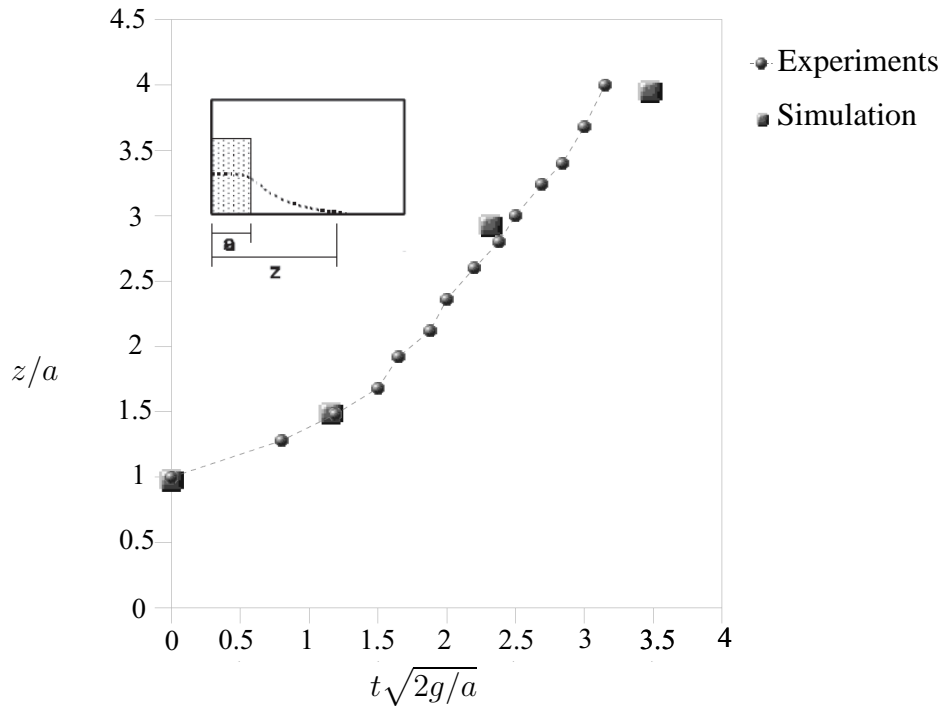
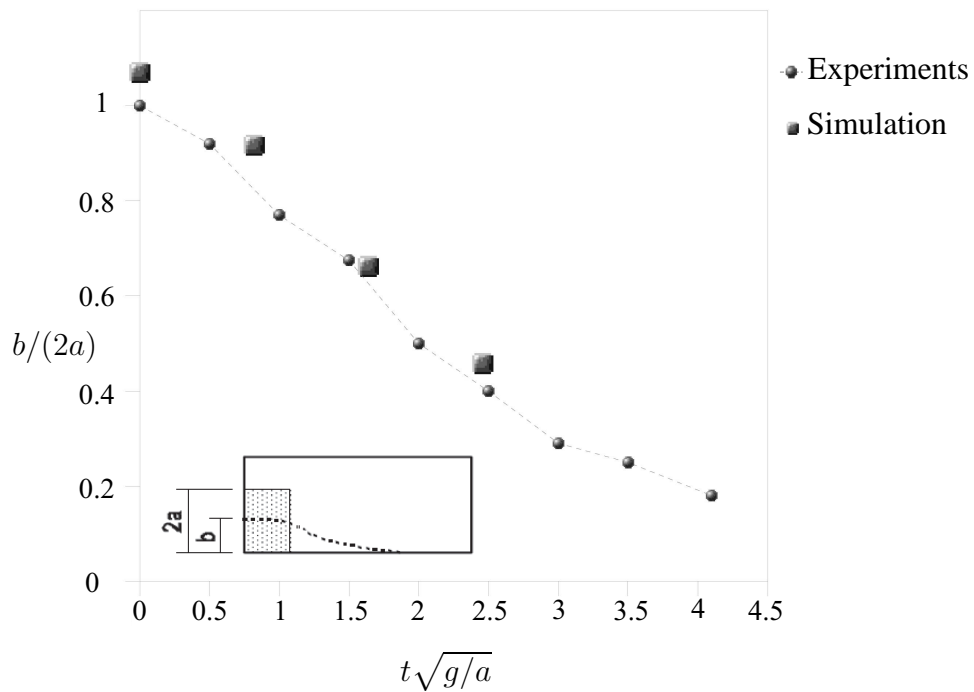Figure 4: Position of the leading edge versus time

Figure 5: Height of the collapsing water column versus time

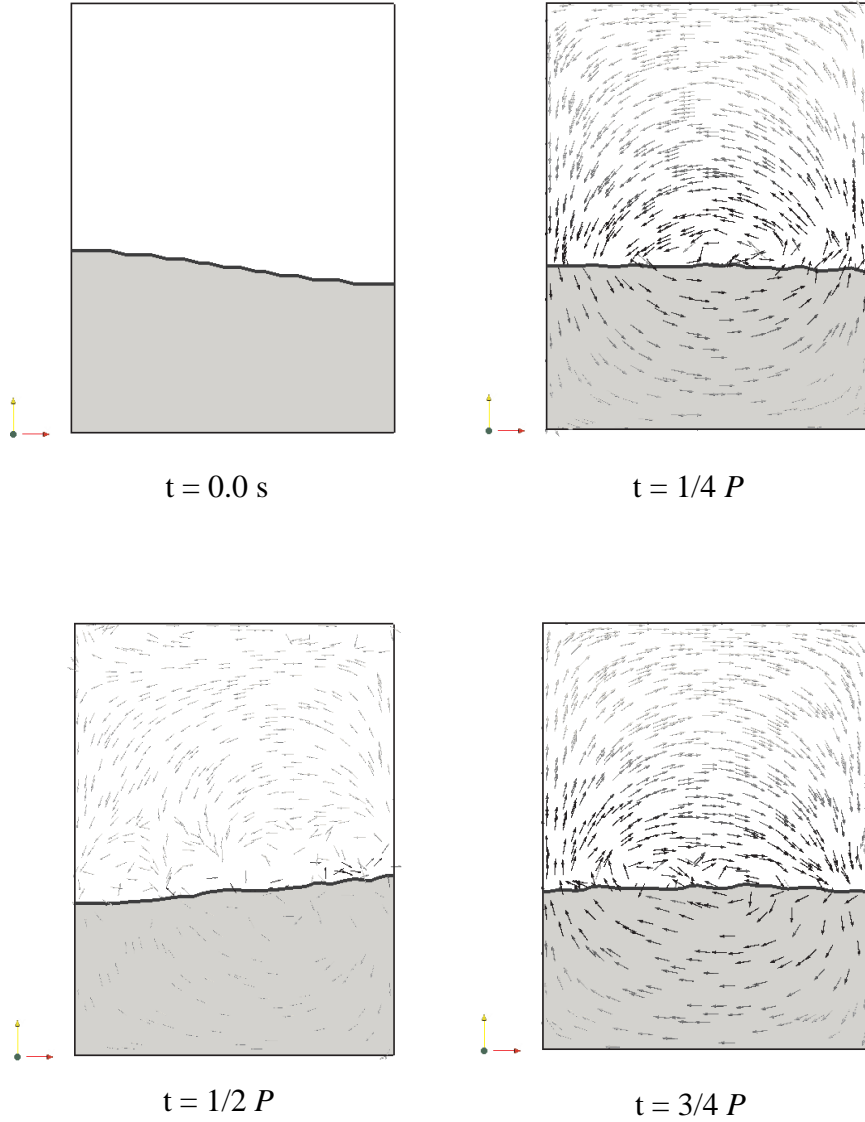with the wave number k and the average fluid depth h. The numerical results are shown in Figure 6.

Figure 6: Wave position and velocity vectors for the first period of the sloshing

Raad[9] introduced a definition for the temporal error which is defined as

$$\epsilon_t = 100 \frac{(t_s - t_t)}{t_t} \tag{40}$$

with the theoretical time t_t calculated as the amount of periods multiplied by the period time and the time gained from the simulation t_s. The time of the simulations represents the time

Theoretical Time	Raad[9]	Ubbink[8]	Coupled Approach
2 P	-0.44	0.0	-0.37
4 P	-0.39	-0.75	-0.19

Table 1: Temporal error in %

when the interface reaches its highest point at the left boundary. The temporal error for the first two even periods are presented in Table 1.

As can be seen in Table 1, the results of the coupled solution approach show very good agreement with the data from literature[8] for the first two even periods. However, the damping effect of the discretisation becomes significant starting at the 5th period which makes an evaluation for higher periods impossible.

4.3 Dam break with three phases in 3d

A dam break case with three phases in 3d was considered to test the behaviour of the presented method for more than two phases. The variety of industrial applications with more than two phases is numerous and the applicability of the presented method for more than two phases has been shown in the theoretical part. However such problems have not yet been subject to extensive tests, which causes the absence of applicable validation data in literature. Therefore the following test case can merely be seen as a proof of concept and is set up as an extension of the dam break case presented in 2d with two phases. Due to the gravitational acceleration, two water columns collapse as presented before. The computational domain has a length, width and height of 0.584 m and initially the water columns are positioned at the left and the right boundary of the domain. Slightly appart from the middle of the domain there is a small obstacle placed in the way of the wave fronts which leads to a mixing of the two liquid phases due to the asymetric arrangement. The simulation results are shown in Figure 7.

5 CONCLUSIONS

A coupled pressure based solution algorithm was developed and validated on test cases. The calculated results agree well with experimental data taken from literature. The test cases, however, have also revealed that the implicit coupling of the equations seriously weakens the diagonal dominance of the system matrix, which has a great impact on the stability of the simulation results. Therefore further effort has to be put into the development of suitable solvers for systems with block matrices. Moreover, the algorithm needs to be enhanced to capture multiphase flow where the surface tension effects are dominant.

ACKNOWLEDGMENT

t = 0.0 s

t = 0.1 s

t = 0.5 s

t = 1.25 s

t = 1.5 s

t = 2.0 s
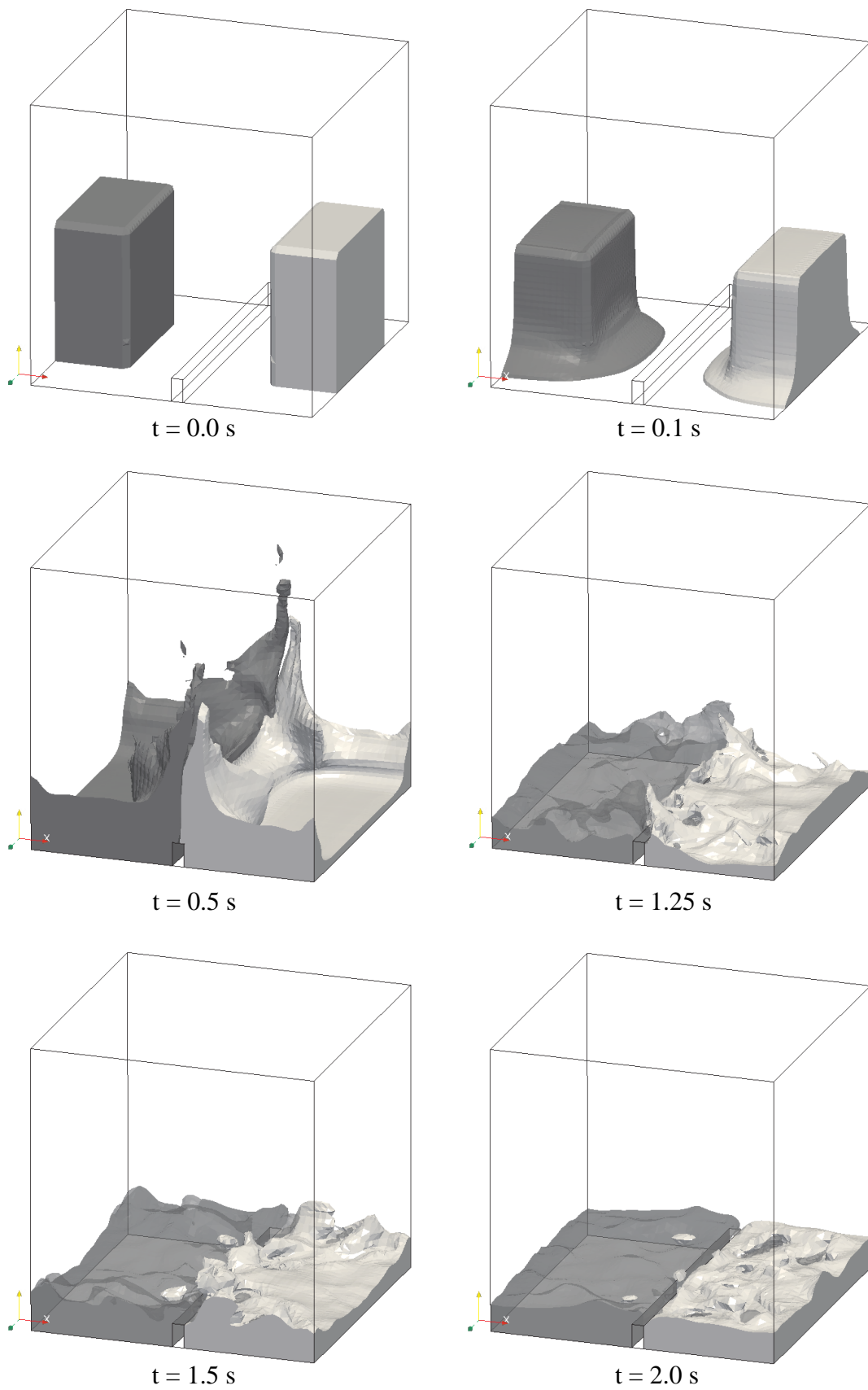
Figure 7: Dam break in 3d for t = 0 s, t = 0.1 s, t = 0.5 s, t = 1.25 s, t = 1.5 s and t = 2.0 s

REFERENCES

[1] I. Clifford, H. Jasak, The Application of a Multi-Physics Toolkit to Spatial Reactor Dynamics. *International Conference on Mathematics, Computational Methods and Reactor Physics* (2009).

[2] J. U. Brackbill, D. B. Kothe and C. Zemnach, A Continuum Method for Modelling Surface Tension. *Journal of Computational Physics* **100**, (1992), pp. 335-354.

[3] H. G. Weller. Derivation modelling and solution of the conditionally averaged two-phase flow equations. Technical Report TR/HGW/02, Nabla Ltd, 2002.

[4] H. Rusche, Computational Fluid Dynamics of Dispersed Two-Phase Flows at High Phase Fractions. PhD Thesis, Imperial College of Science, Technology & Medicine (2002).

[5] J. H. Ferziger, M. Peric, Computational methods for fluid dynamics. Springer Verlag, Berlin (1996).

[6] S. V. Patankar, D. B. Spalding, A calculation procedure for heat, mass and momentum transfer in three-dimensional parabolic flows. *Int. J. Heat Mass Transfer* **15**, (1972), pp. 1787-1806.

[7] S. Koshizuka, H. Tamako, Y. Oka, A Particle method for Incompressible Flow with Fluid Fragmentation. *Computational Fluid Dynamics Journal* **4** (1995), pp. 29-46.

[8] O. Ubbink, Numerical Prediction of Two Fluid Systems with Sharp Interfaces. PhD Thesis, Imperial College of Science, Technology & Medicine (1997).

[9] P. E. Raad, S. Chen, D.B. Johnson, The Introduction of Micro Cells to Treat Pressure Free Surface Fluid Flow Problems. *Journal of Fluids Engineering* **117** (1995), pp. 683-690.

[10] I. Tadjbakhsh, J.B. Keller, Standing Surface Waves of Finite Amplitude. *Journal of Fluid Mechanics* **8** (1960), pp. 442-451.